Green Chemistry

PAPER

View Article Online
View Journal

Cite this: DOI: 10.1039/c9gc03646f

Thermally regulated molybdate-based ionic liquids toward molecular oxygen activation for one-pot oxidative cascade catalysis†

Zhibin Song, [a] Wei Huang,[a] Yan Zhou,[a] Zi-Qi Tian, [a,b] Zhang-Min Li[a] and Duan-Jian Tao *[a]

One-pot oxidative cascade catalysis plays a central role in the synthesis of key pharmaceutical and industrial molecules. Although ionic liquids are one of the most promising solvents and reaction media, the breakthrough of their catalysis in aerobic oxidation is very challenging due to the difficulty in the direct activation of molecular oxygen. Herein, a family of novel thermally regulated molybdate-based ionic liquids (Mo-ILs) has been designed and developed for the first time toward molecular oxygen activation for highly efficient tandem oxidative catalysis. Three diverse one-pot oxidative cascade processes for the syntheses of various flavones, imines, and benzyl benzoates were achieved with good to excellent yields using the Mo-IL $[Bmim]_2[MoO_4]$ as a catalyst under air conditions. The results of spectroscopic investigations and quantum-chemical calculations further demonstrated that a thermally regulated proton migration between the cation [Bmim] and anion $[MoO_4]$ was the key to forming N-heterocyclic carbene and thereby to effortlessly promoting the generation of $^{\bullet}O_2^-$ active species from molecular oxygen, which results in excellent catalytic performance in these three aerobic tandem oxidations. Our work extends the application area of ILs as the sole catalyst to one-pot aerobic oxidative cascade catalysis, which could have pronounced implications in future work.

Received 23rd October 2019,
Accepted 15th November 2019

DOI: 10.1039/c9gc03646f

rsc.li/greenchem

Introduction

Task-specific ionic liquids (TSILs), as a new type of green solvent and efficient catalyst, have been studied widely owing to their unique properties, including excellent solubility, high thermal stability, and virtually unlimited tunability.[1–5] Recently, carbanion-functionalized ILs were prepared and developed for highly efficient carbon monoxide capture and subsequent conversion.[6] SO_3H-functionalized ILs can also be used for dissolution and *in situ* catalytic transformation of biomass resources.[7–9] These achievements prove that TSILs play an exemplary role in improving catalytic efficiency and performing multi-step processes in one-pot.

One-pot oxidative cascade catalysis for the construction of complex and important molecules is extremely attractive and highly desirable in contemporary chemical science, since it can avoid the isolation and purification of intermediates and also reduce chemical waste.[10–14] However, as a result of the catalytic application area of IL catalysts mainly in acid–base catalysis,[15–19] the IL simply acts as a medium or additive in such a one-pot oxidative process to date. There is scarcely any study concerning aerobic oxidative cascade catalysis by the IL catalyst, especially using molecular oxygen as the terminal oxidant.[20,21] The dilemma is that the state-of-the-art ILs as the sole catalyst can hardly activate molecular oxygen for a highly efficient aerobic oxidation reaction so far. In view of this, it is very challenging and highly desirable to develop novel ILs for aerobic cascade catalysis, involving the activation of molecular oxygen under mild conditions.

In this article, we designed and prepared a series of novel thermally regulated molybdate-based ionic liquids (Mo-ILs). The Mo-ILs could be used as superior catalysts toward molecular oxygen activation for highly efficient tandem oxidative reactions for the first time. As a result, three diverse one-pot oxidative cascade processes for the synthesis of flavone from 2′-hydroxyacetophenone with benzaldehyde, imine from aniline with benzyl alcohol, and benzyl benzoate from benzyl alcohol were achieved with excellent yields, respectively. The results of spectroscopic investigations and quantum-chemical

[a]*Key Laboratory of Functional Small Organic Molecule, Ministry of Education, College of Chemistry and Chemical Engineering, Jiangxi Normal University, Nanchang 330022, China. E-mail: djtao@jxnu.edu.cn*
[b]*Ningbo Institute of Materials Technology & Engineering, Chinese Academy of Sciences, Ningbo, Zhejiang 315201, China*

†Electronic supplementary information (ESI) available: Additional characterization and reaction results. See DOI: 10.1039/c9gc03646f

calculations further showed that such excellent catalytic activities arise from a thermally-induced proton migration interaction between [Bmim] and [MoO_4] in the Mo-IL [Bmim]$_2$[MoO_4] catalyst, and thereby promote an effortless generation of $^{\bullet}O_2^-$ active species.

Results and discussion

Catalytic performance of Mo-ILs

The chemical structures of six Mo-ILs designed in this work are shown in Scheme 1. These six Mo-ILs are prepared by neutralization with hydroxide and molybdic acid. The structures of Mo-ILs were confirmed by nuclear magnetic resonance (NMR), infrared spectroscopy (IR), and mass spectrometry. The characterization results are presented in the ESI (Fig. S1, S2, and Table S1†). The water content of these Mo-ILs was also determined by a Karl Fisher titration and found to be less than 0.1 wt%.

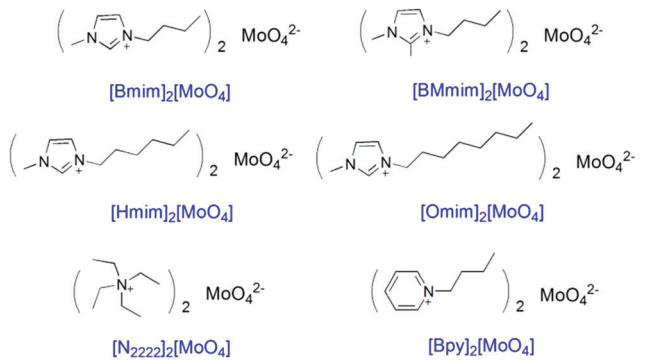

Scheme 1 Structures of the anions and cations in Mo-ILs.

Flavones, also named 2-phenylchromones, are very important oxygen-containing heterocycles, which are abundant in nature, especially in plants.[23,24] As a member of the flavonoid family,[25] flavones exhibit diverse and superior biological activities based on the substitution pattern, particularly in inhibiting oxidative-stress related diseases.[26–28] Also the development of new efficient synthetic procedures of flavones will provide convenient tool for structural modification and structure–activity relationship investigation.[29] As one of the most popular procedures for the synthesis of flavones,[30] the chalcone route involves a base-catalyzed Claisen–Schmidt condensation, cyclization and further oxidative dehydrogenation,[21] which is a promising way to realize multi-step processes in one-pot *via* oxidative cascade catalysis. Therefore, we employed these Mo-ILs as the sole catalysts to achieve one-pot synthesis of flavone from the reaction of 2′-hydroxyacetophenone and benzaldehyde (Table 1).

Surprisingly, it was indicated that three imidazolium Mo-ILs showed very high catalytic activities for one-pot synthesis of flavone under an air atmosphere *via* the base-catalyzed Claisen–Schmidt condensation and cyclization as well as subsequent oxidative tandem dehydrogenation. A 98% yield of **5a** flavone was then obtained using [Bmim]$_2$[MoO_4] as the catalyst after screening of the reaction conditions (Table 1, entry 1 and Table S2†). Notably, the 3-alkyl substituent of the imidazolium moiety hardly has any effect on the good performance of imidazolium Mo-ILs (Table 1, entries 2 and 3). Nonetheless, [N_{2222}]$_2$[MoO_4] and [Bpy]$_2$[MoO_4] without the imidazolium cation showed poor performance for **5a** flavone. The catalyst K_2MoO_4 showed no catalytic activity while the IL [Bmim]$_2$[SA] without a molybdate anion also induced a very low conversion

Table 1 Aerobic oxidative tandem reactions for the synthesis of flavone catalyzed by various Mo-IL catalysts[a]

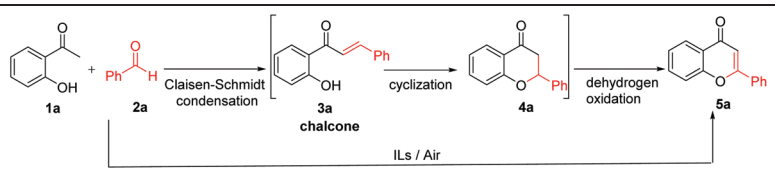

Entry	Catalyst	Conversion % of **2a**	Yield % of **3a**	Yield % of **4a**	Yield % of **5a**
1	[Bmim]$_2$[MoO_4]	98	n.d.	n.d.	98 (94)[b]
2	[Hmim]$_2$[MoO_4]	97	3	2	92
3	[Omim]$_2$[MoO_4]	96	2	4	90
4	[N_{2222}]$_2$[MoO_4]	86	28	45	13
5	[Bpy]$_2$[MoO_4]	20	2	14	4
6	K_2MoO_4	<1	n.d.	n.d.	n.d.
7[c]	[Bmim]$_2$[SA]	15	11	4	n.d.
8[d]	[Bmim]$_2$[MoO_4]	n.d.	n.d.	n.d.	n.d.
9	[BMmim]$_2$[MoO_4]	97	25	54	18
10[e]	[Bmim]$_2$[MoO_4]	20	<5	15	<2
11[f]	[Bmim]$_2$[MoO_4]	15	<5	10	<1

[a] Reaction conditions: **1a** (2.0 mmol), **2a** (2.0 mmol), [Bmim]$_2$[MoO_4] (0.6 mmol), *n*-hexanol (1 mL), 140 °C, 3 h, under an air atmosphere, determined by GC and GC-MS analysis. [b] Yield after five recycles. [c] [SA]: succinate. [d] Under an argon atmosphere. [e] TEMPO (5 equiv.). [f] Benzoquinone (5 equiv.).

of **2a** and a poor yield of **5a** proving that the synergistic catalysis of the imidazolium moiety and molybdate anion may result in an excellent yield of **5a** *via* an aerobic oxidative cascade reaction.

In addition, it is well known that molybdate has certain oxidation ability. Thus, we investigated the reusability of $[Bmim]_2[MoO_4]$. As shown in Fig. S3,† the $[Bmim]_2[MoO_4]$ catalyst can retain high reactivity for up to five cycles, showing its good reusability under air conditions. The recycled catalyst was also characterized by Raman spectra. The main characteristic peaks of the reused $[Bmim]_2[MoO_4]$ were consistent with those of a fresh catalyst (Fig. S4†). However, the trace of **5a** was hardly detected in the recycle test under an argon atmosphere (Table 1, entry 8), implying O_2 as the terminal oxidant under an ambient atmosphere. The direct oxidative dehydrogenation of **4a** under standard conditions by $[Bmim]_2[MoO_4]$ was also conducted. The GC yield of **5a** was 89% in this direct oxidative reaction (Scheme S1).†

Probing into the catalysis of $[Bmim]_2[MoO_4]$

According to the literature reports,[31–33] imidazolium-based ILs can lead to the formation of N-heterocyclic carbene. To determine the effect of imidazolium on the catalytic activity of $[Bmim]_2[MoO_4]$, we speculated that the H at the C-2 position of [Bmim] plays a key role in the catalysis of $[Bmim]_2[MoO_4]$ involving a proton transfer to generate N-heterocyclic carbene. To explore this possibility, the controlled Mo-IL $[BMmim]_2[MoO_4]$ was prepared through the substitution of the hydrogen atom by the methyl group at the C-2 position of imidazolium cations and examined for the one-pot synthesis of flavone. As was expected, **4a** was the major product and only 18% yield of **5a** was thus obtained (Table 1, entry 9). This result verified the probable responsibility of H at the C-2 position of [Bmim] for highly efficient synthesis of **5a**. Moreover, the temperature-dependent ^1H and ^{13}C NMR experiments at 25 °C and 70 °C were further performed to observe a proton transfer process in $[Bmim]_2[MoO_4]$ (Fig. 1, S5, and S6†). When the temperature was up to 70 °C, the signal of H (at 9.84 ppm) at the C-2 position of imidazolium reduced dramatically, demonstrating a possible thermally-induced proton transfer between the imidazolium cation and molybdate anion in $[Bmim]_2[MoO_4]$. Accordingly, a series of new peaks appeared in the ^{13}C NMR spectra from the imidazolium cation at 70 °C, which also indicated the possible occurrence of proton migration in $[Bmim]_2[MoO_4]$.

Subsequently, an improved Raman spectroscopy to monitor the reaction system with $[Bmim]_2[MoO_4]$ was also performed at 25 °C and 70 °C, respectively (Fig. 2). In the Raman spectra of $[Bmim]_2[MoO_4]$ at 25 °C, a typical characteristic peak was observed at 890 cm^{-1}, which can be assigned to the stretching vibration of Mo–O in the anion $[MoO_4]$.[34,35] At the temperature of 70 °C, the Mo–O vibrational frequency of $[Bmim]_2[MoO_4]$ in the reaction mixture was obviously blue-shifted to 950 cm^{-1}. This observation was also in good agreement with the simulation results for the Raman spectroscopy of various Mo species based on density functional theory (DFT) calculations (Fig. 3 and Table S3†).[36,37] It is shown in Fig. 3 that combination with protons can apparently increase the frequency of the Mo–O bond to about 950 cm^{-1}, suggesting that the proton transfer to form $[HMoO_4]$ is responsible for the change in the Raman spectra. Thus, on the basis of these results, it is validated that a proton migration between [Bmim] and $[MoO_4]$ was indeed observed in $[Bmim]_2[MoO_4]$, thereby forming the complex of N-heterocyclic carbene, which accounts for the outstanding catalytic efficiency in such aerobic cascade oxidation.

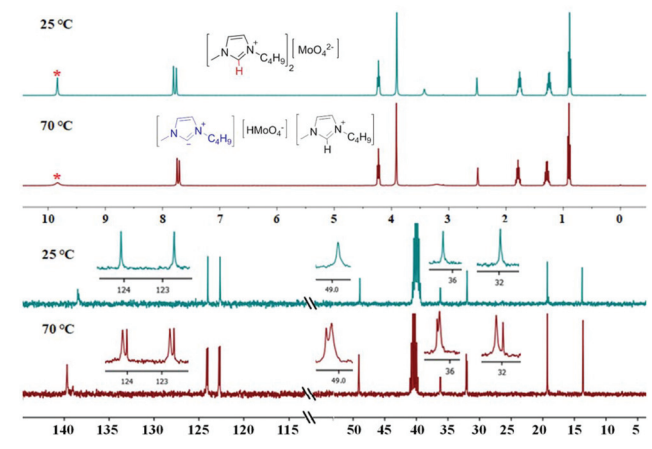

Fig. 1 ^1H and ^{13}C NMR spectra of $[Bmim]_2[MoO_4]$ at 25 °C and 70 °C.

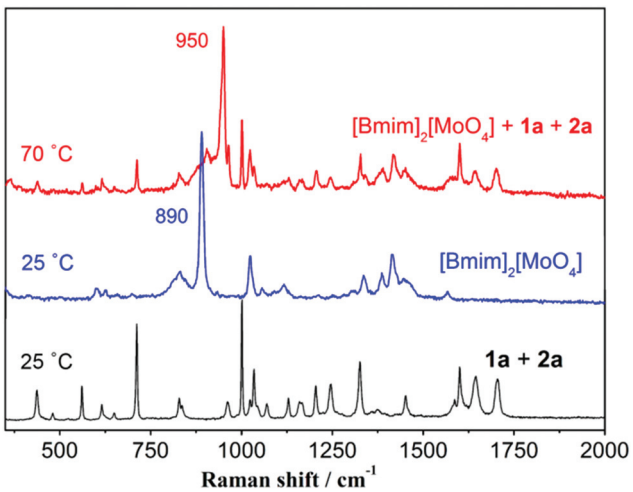

Fig. 2 Raman spectra of the reaction system with $[Bmim]_2[MoO_4]$ at 25 °C and 70 °C.

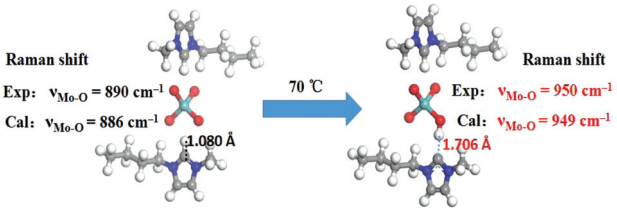

Fig. 3 The comparison of the experimental and calculated Raman spectra of $[Bmim]_2[MoO_4]$.

The mechanism of O_2 activation

In order to further investigate whether reactive oxygen species (ROS) were generated in the aerobic oxidative tandem reaction for one-pot synthesis of **5a**, scavenger experiments over the $[Bmim]_2[MoO_4]$ catalyst were carried out by employing 2,2,6,6-tetramethyl-1-piperidinyloxy (TEMPO) and 1,4-benzoquinone (BQ) as radical scavengers (Table 1, entries 10 and 11). It was observed that the addition of TEMPO and BQ significantly suppressed the conversion of **2a** and resulted in a very low yield of **5a**, implying a possible radical reaction process and that ROS are the dominant reactive species accounting for this oxidative cascade reaction. An electron paramagnetic resonance (EPR) experiment was then performed to directly detect ROS species with the addition of a free-radical spin-trapping agent 5,5-dimethyl-1-pyrroline *N*-oxide (DMPO). An instant EPR spectrum was observed with $[Bmim]_2[MoO_4]$ in *n*-hexanol in the presence of DMPO at 70 °C (Fig. 4). Despite the formation of more than one radical adduct of DMPO, the main spin-trapped product DMPO-OOH can be well identified (a^N = 14 G, a^H = 11.4 G, for simulation details see Fig. S7†), which is obtained from DMPO–$^{\bullet}O_2^-$,[38–42] thus offering conclusive evidence for the promoted generation of $^{\bullet}O_2^-$ in the reaction system with $[Bmim]_2[MoO_4]$. In contrast, the signal of reactive oxygen species was not detected for the blank and common IL $[Bmim][Tf_2N]$. On the basis of these results, we inferred that the $^{\bullet}O_2^-$ radicals are the reactive oxygen species that possess the appropriate oxidation capacity for one-pot synthesis of **5a** over the $[Bmim]_2[MoO_4]$ catalyst.

Why did $[Bmim]_2[MoO_4]$ promote O_2 effortlessly to generate $^{\bullet}O_2^-$ active species for efficient aerobic cascade oxidation? To illustrate the underlying mechanism, we also employed DFT calculations at the UB3LYP/6-31+G(d) level to investigate the interaction between $[Bmim]_2[MoO_4]$ and O_2. First, the free energy profile of proton transfer from a cation to $[MoO_4]$ is depicted in Fig. 5a, showing that the energy barrier for N-heterocyclic carbene generation is only 2.26 kcal mol^{-1}. It can be overcome under relatively mild conditions. In $[Bmim][Bmim\text{-}H][HMoO_4]$, the distance between the migrated hydrogen and 2-C is 1.706 Å (Fig. 3), much longer than the normal C–H covalent bond, implying the formation of carbene species.[37] Also, we suppose that N-heterocyclic carbene can activate oxygen and further promote aerobic oxidation. Herein the frontier orbitals of the [Bmim] cation, [Bmim-H] radical and oxygen molecules in the ground state are studied to understand the role of carbene radicals. Fig. 5b illustrates that the HOMO of the [Bmim-H] radical is significantly higher than that of the [Bmim] cation, thus also much closer to the unoccupied β orbital of oxygen. The narrowed energy difference between the HOMO of imidazolium species and the unoccupied orbital of oxygen facilitates charge transfer, resulting in the generation of an active $^{\bullet}O_2^-$ radical that further participates in the oxidative reaction. Overall, on the basis of the observed results, a plausible catalytic mechanism of $[Bmim]_2[MoO_4]$ for an efficient aerobic cascade reaction can be proposed, which involves a proton migration interaction between [Bmim] and $[MoO_4]$ and thereby promotes an effortless generation of $^{\bullet}O_2^-$ active species between [Bmim-H] carbene and O_2.

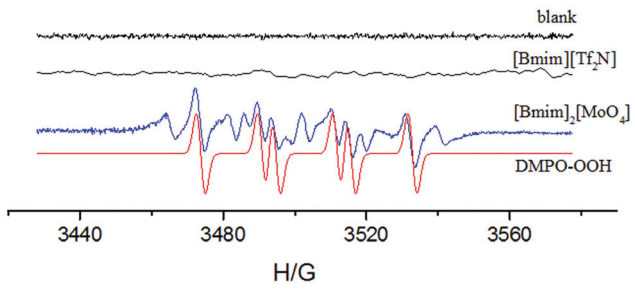

Fig. 4 EPR spectra of different samples in the presence of DMPO.

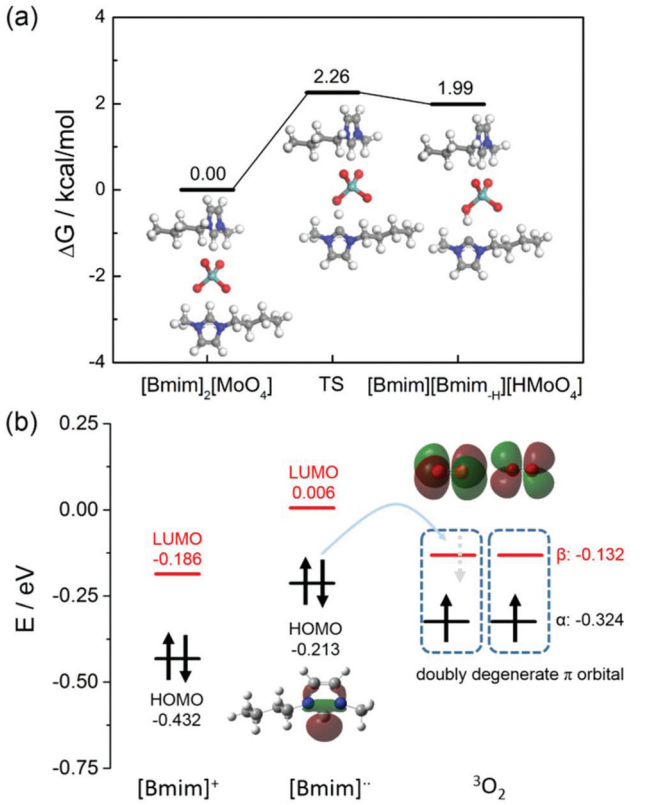

Fig. 5 (a) Free energy profile of the process of proton migration. (b) Calculated frontier orbitals of [Bmim] cation, [Bmim-H] carbene, and triplet oxygen.

The applicability of $[Bmim]_2[MoO_4]$

More importantly, the applicability of $[Bmim]_2[MoO_4]$ was investigated for catalyzing other two types of aerobic cascade reactions (Scheme 2). It was demonstrated that the aerobic tandem reaction of aniline with benzyl alcohol was performed to produce imine with 91% yield. Benzyl alcohol could be converted to benzyl benzoate *via* one-step oxidative esterification with a relatively good yield. Furthermore, various flavones, imines, and benzyl benzoate derivatives could also be obtained

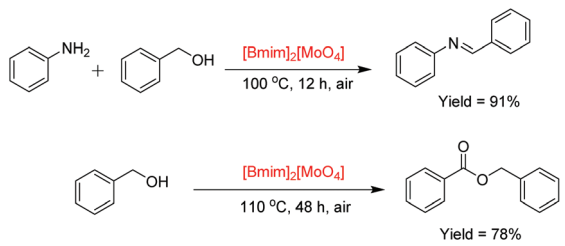

Scheme 2 The other two aerobic cascade reactions catalyzed by the Mo-IL $[Bmim]_2[MoO_4]$.

with good to excellent yields *via* these three one-pot oxidative reaction processes (Tables S4–S6†).

Conclusions

In summary, we have designed and developed novel thermally regulated Mo-ILs toward molecular oxygen activation for highly efficient one-pot oxidative cascade catalysis. The Mo-IL $[Bmim]_2[MoO4]$ can be used as a superior catalyst for three diverse one-pot cascade aerobic oxidation processes, in which the syntheses of flavone from 2′-hydroxyacetophenone with benzaldehyde, imine from aniline with benzyl alcohol, and benzyl benzoate from benzyl alcohol were achieved with good to excellent yields, respectively. Quantum-chemical calculations and characterization techniques demonstrated that the proton migration in $[Bmim]_2[MoO_4]$ is the key to generate N-heterocyclic carbene and thereby to effortlessly promote the generation of $^{\bullet}O_2^-$ active species from molecular oxygen, which accounts for the excellent catalytic performance in various aerobic tandem oxidations. The current work extends the application area of ILs to the field of aerobic oxidation catalysis, which could have pronounced implications in future work.

Experimental

Materials

Molybdic acid (H_2MoO_4, 99%), potassium molybdate (K_2MoO_4, 99%), and 2′-hydroxyacetophenone (99%) were purchased from Adamas (Shanghai). 1-Butyl-3-methylimidazolium bromide ([Bmim]Br, 99%), 1-hexyl-3-methylimidazolium bromide ([Hmim]Br, 99%), 1-octyl-3-methylimidazolium bromide ([Omim]Br, 99%), 1-butyl-2-methyl-3-methylimidazolium bromide ([BMmim]Br, 99%), and 1-butylpyridinium bromide ([Bpy]Br, 99%) were obtained from the Centre of Green Chemistry and Catalysis, LICP, CAS. All the other chemicals were obtained in the highest purity grade possible and used as received.

Preparation of Mo-ILs

A typical procedure for the preparation of the IL $[Bmim]_2[MoO_4]$ is described as follows: a solution of 1-butyl-3-methylimidazolium hydroxide ([Bmim]OH) in ethanol was obtained from [Bmim]Br using the anion-exchange resin method according to the previous work,[6] and an equimolar amount of H_2MoO_4 was added to the ethanol solution of [Bmim]OH. Then the mixture was stirred at room temperature for 5 h. Subsequently, the as-prepared IL $[Bmim]_2[MoO_4]$ was dried and obtained under vacuum at 90 °C for 48 h to eliminate the solvent and traces of impurities. In addition, the other Mo-ILs $[Hmim]_2[MoO_4]$, $[Omim]_2[MoO_4]$, $[BMmim]_2[MoO_4]$, and $[Bpy]_2[MoO_4]$ were synthesized in a similar manner to that of $[Bmim]_2[MoO_4]$.

Mo-IL characterization analysis

The Mo-IL catalysts were extensively characterized using ^{1}H NMR and ^{13}C NMR (100 MHz) spectroscopy, Fourier transform infrared (FT-IR) spectroscopy, Raman spectroscopy, thermogravimetric analysis (TGA), electrospray ionization mass spectrometry (ESI-MS), and elemental analysis. ^{1}H NMR (400 MHz) and ^{13}C NMR (100 MHz) spectra were recorded on a Bruker Avance 400 spectrometer. FT-IR spectra were recorded on a Nicolet 6700 spectrometer. Raman spectroscopy was performed on a LabRAM HR spectrometer with an excitation wavelength at 632 nm with 3 cm^{-1} spectral resolution. TGA was carried out on a PerkinElmer Diamond TG/DTA apparatus under a nitrogen atmosphere. The initial oven temperature was set at 25 °C, and then ramped at 10 °C min^{-1} to 600 °C. ESI-MS analysis of Mo-ILs was carried out on an Agilent1290/maXis impact (Bruker). The samples were injected as dilute solutions in methanol, and both positive and negative ions were measured with an m/z range of 50 to 600. The CHN elemental contents of Mo-based ILs were measured on an Elementar Vario El III instrument, while molybdenum contents in the samples were determined by inductively coupled plasma optical emission spectrometry (ICP-OES) using an Agilent 720 instrument. The water content of the resulting Mo-ILs was found to be less than 0.15 wt% as determined by the Karl Fisher titration. The residual bromide content of these Mo-ILs was also checked to be less than 500 ppm by the Mohr titration. EPR spectra were recorded on a Bruker E580 spectrometer.

One-pot catalytic aerobic tandem oxidation

In a typical run, 2′-hydroxyacetophenone (2 mmol), benzaldehyde (2 mmol), Mo-IL catalyst (0.6 mmol), and *n*-hexanol (1 mL) were charged in a 10 mL round-bottomed flask equipped with a magnetic stirrer. The reaction was stirred at 140 °C for 3 h under an air atmosphere. After the reaction was complete, the reactor was cooled down. About 0.2 mL of liquid sample was diluted with ethanol and identified by gas chromatography-mass spectrometry (GC-MS) (Thermo Trace 1300 GC-ISQ). The products were further quantified by a GC-FID (Agilent 7890B) equipped with a capillary column HP-5 (methyl polysiloxane, 30 m × 0.32 mm × 1 μm). Trimethylbenzene was used as an internal standard to quantify the products. The procedures for the synthesis of benzanilides and benzyl benzoates were also similar to that of flavones.

Recycling of the Mo-IL catalyst

After the reaction was complete, the reaction mixture was extracted with 15 mL ethyl acetate and 10 mL deionized water. The system thus formed a liquid–liquid biphase, and the aqueous phase containing a Mo-IL catalyst could be easily separated by simple decantation. After that, the Mo-IL catalyst was further kept in a vacuum oven at 80 °C for 12 h to remove water and the residual reactants prior to reuse in the next run. Subsequently, the organic phase was concentrated under vacuum and then purified by flash chromatography (petroleum ether : ethyl acetate = 20 : 1) to afford the corresponding product.

Computational details and theoretical methods

The structures of all the studied molecules were determined using the Gaussian 09 software package.[22] The B3LYP hybrid functional was employed with LANL2DZ pseudo potential for Mo and the 6-31+G(d) basis set for other elements. An unrestricted method was used for the systems containing radical and triplet species. Frequency calculations were further performed to confirm that all the optimized structures are local minima with no imaginary frequency.

Conflicts of interest

There are no conflicts to declare.

Acknowledgements

We thank the National Natural Science Foundations of China (No. 21606116, 31570560, 21566011), the Jiangxi Province Sponsored Programs for Distinguished Young Scholars (No. 20162BCB23026), the Natural Science Foundations of Jiangxi Province (No. 20192ACBL20025), and the Science & Technology Programs of Jiangxi Province Department of Education (No. GJJ160272) for financial support.

Notes and references

1 Z. M. Li, Z. P. Cai, Q. Zeng, T. Zhang, L. J. France, C. H. Song, Y. Q. Zhang, H. Y. He, L. L. Jiang, J. X. Long and X. H. Li, *Green Chem.*, 2018, **20**, 3743–3752.
2 G. Wang, Z. Li, C. Li and S. Zhang, *Green Energy Environ.*, 2019, **4**, 293–299.
3 C. Dai, Z. Lei and B. Chen, *AIChE J.*, 2017, **63**, 1792–1798.
4 W. Hui, Y. Zhou, Y. Dong, Z. J. Cao, F. Q. He, M. Z. Cai and D. J. Tao, *Green Energy Environ.*, 2019, **4**, 49–55.
5 E. N. Kusumawati and T. Sasaki, *Green Energy Environ.*, 2019, **4**, 180–189.
6 D. J. Tao, F. F. Chen, Z. Q. Tian, K. Huang, S. M. Mahurin, D. Jiang and S. Dai, *Angew. Chem., Int. Ed.*, 2017, **56**, 6843–6847.
7 J. Long, W. Lou, L. Wang, B. Yin and X. Li, *Chem. Eng. Sci.*, 2015, **122**, 24–33.
8 J. Long, X. Li, L. Wang and N. Zhang, *Sci. China: Chem.*, 2012, **55**, 1500–1508.
9 A. Pinkert, K. N. Marsh, S. S. Pang and M. P. Staiger, *Chem. Rev.*, 2009, **109**, 6712–6728.
10 K. C. Nicolaou, D. J. Edmonds and P. G. Bulger, *Angew. Chem., Int. Ed.*, 2006, **45**, 7134–7186.
11 B. Yang, Y. Qiu and J. E. Bäckvall, *Acc. Chem. Res.*, 2018, **51**, 1520–1531.
12 D. Zhang, J. Liu, A. Córdova and W. W. Liao, *ACS Catal.*, 2017, **7**, 7051–7063.
13 Y. Qiu, B. Yang, C. Zhu and J. E. Bäckvall, *J. Am. Chem. Soc.*, 2016, **138**, 13846–13849.
14 V. R. Naidu, D. Posevins, C. M. R. Volla and J. E. Bäckvall, *Angew. Chem., Int. Ed.*, 2017, **56**, 1590–1594.
15 C. Dai, J. Zhang, C. Huang and Z. Lei, *Chem. Rev.*, 2017, **117**, 6929–6983.
16 V. I. Parvulescu and C. Hardacre, *Chem. Rev.*, 2007, **107**, 2615–2665.
17 Q. Zhang, H. Y. Yuan, N. Fukaya, H. Yasuda and J. C. Choi, *Green Chem.*, 2017, **19**, 5614–5624.
18 Y. Zhou, W. Huang, X. S. Chen, Z. B. Song and D. J. Tao, *Catal. Lett.*, 2015, **145**, 1830–1836.
19 Z. Y. Yu, M. Y. Chen, J. X. He, D. J. Tao, J. J. Yuan, Y. Y. Peng and Z. B. Song, *Mol. Catal.*, 2017, **434**, 134–139.
20 Z. Shi, C. Zhang, C. Tang and N. Jiao, *Chem. Soc. Rev.*, 2012, **41**, 3381–3430.
21 T. Yatabe, X. Jin, K. Yamaguchi and N. Mizuno, *Angew. Chem., Int. Ed.*, 2015, **54**, 13302–13306.
22 M. J. Frisch, G. W. Trucks, H. B. Schlegel, G. E. Scuseria, M. A. Robb, J. R. Cheeseman, G. Scalmani, V. Barone, B. Mennucci, G. A. Petersson, H. Nakatsuji, M. Caricato, X. Li, H. P. Hratchian, A. F. Izmaylov, J. Bloino, G. Zheng, J. L. Sonnenberg, M. Hada, M. Ehara, K. Toyota, R. Fukuda, J. Hasegawa, M. Ishida, T. Nakajima, Y. Honda, O. Kitao, H. Nakai, T. Vreven, J. A. E. Montgomery, J. Peralta, F. Ogliaro, M. Bearpark, J. J. Heyd, E. Brothers, K. N. Kudin, V. N. Staroverov, R. Kobayashi, J. Normand, K. Raghavachari, A. Rendell, J. C. Burant, S. S. Iyengar, J. Tomasi, M. Cossi, N. Rega, J. M. Millam, M. Klene, J. E. Knox, J. B. Cross, V. Bakken, C. Adamo, J. Jaramillo, R. Gomperts, R. E. Stratmann, O. Yazyev, A. J. Austin, R. Cammi, C. Pomelli, J. W. Ochterski, R. L. Martin, K. Morokuma, V. G. Zakrzewski, G. A. Voth, P. Salvador, J. J. Dannenberg, S. Dapprich, A. D. Daniels, O. Farkas, J. B. Foresman, J. V. Ortiz, J. Cioslowski and D. J. Fox, *Gaussian09, RevisionD.01*, Gaussian, Inc., Wallingford, CT, 2009.
23 A. R. Jassbi, S. Zare, M. Asadollahi and M. C. Schuman, *Chem. Rev.*, 2017, **117**, 12227–12280.
24 M. H. Pan and C. T. Ho, *Chem. Soc. Rev.*, 2008, **37**, 2558–2574.
25 A. Crozier, I. B. Jaganath and M. N. Clifford, *Nat. Prod. Rep.*, 2009, **26**, 1001–1043.

26 M. Singh, M. Kaur and O. Silakari, *Eur. J. Med. Chem.*, 2014, **84**, 206–239.
27 A. Chanet, D. Milenkovic, C. Manach, A. Mazur and C. Morand, *J. Agric. Food Chem.*, 2012, **60**, 8809–8822.
28 P. G. Pietta, *J. Nat. Prod.*, 2000, **63**, 1035–1042.
29 R. Kshatriya, V. P. Jejurkar and S. Saha, *Tetrahedron*, 2018, **74**, 811–833.
30 K. I. Oyama, K. Yoshida and T. Kondo, *Curr. Org. Chem.*, 2011, **15**, 2567–2607.
31 L. S. Ott, M. L. Cline, M. Deetlefs, K. R. Seddon and R. G. Finke, *J. Am. Chem. Soc.*, 2005, **127**, 5758–5759.
32 H. Rodríguez, G. Gurau, J. D. Holbrey and R. D. Rogers, *Chem. Commun.*, 2011, **47**, 3222–3224.
33 N. M. A. N. Daud, E. Bakis, J. P. Hallett, C. C. Weber and T. Welton, *Chem. Commun.*, 2017, **53**, 11154–11156.
34 H. Tian and I. E. Wachs, *J. Phys. Chem. B*, 2005, **109**, 23491–23499.
35 H. H. Xi, D. Zhou, H. D. Xie, B. He and Q. P. Wang, *J. Am. Ceram. Soc.*, 2015, **98**, 587–593.
36 K. Hamraoui, S. Cristol, E. Payen and J. Paul, *J. Phys. Chem. C*, 2007, **111**, 3963–3972.
37 J. Handzlik and P. Sautet, *J. Phys. Chem. C*, 2008, **112**, 14456–14463.
38 H. Wang, D. Yong, S. Chen, S. Jiang, X. Zhang, W. Shao, Q. Zhang, W. Yan, B. Pan and Y. Xie, *J. Am. Chem. Soc.*, 2018, **140**, 1760–1766.
39 R. A. Burgett, X. Bao and F. A. Villamena, *J. Phys. Chem. A*, 2008, **112**, 2447–2455.
40 P. Lei, C. Chen, J. Yang, W. Ma, J. Zhao; and L. Zhang, *Environ. Sci. Technol.*, 2005, **39**, 8466–8474.
41 H. Wu, Y. Liu, M. Li, Y. Chong, M. Zeng, Y. M. Lo and J. J. Yin, *Nanoscale*, 2015, **7**, 4505–4513.
42 F. Li, L. Xiao, Y. Li, C. Chen and L. Liu, *Chem. Commun.*, 2015, **51**, 11964–11967.